OPEN ACCESS

University of BRISTOL

Kornilov, A., Kennedy, P. D., Aldrovandi, M., Watson, A., Hinz, C., Harless, B., ... O'donnell, V. B. (2019). Revising the structure of a new eicosanoid from human platelets to 8,9-11,12-diepoxy-13-hydroxy-eicosadienoic acid. *Journal of Biological Chemistry*, *294*(23), 9225-9238. https://doi.org/10.1074/jbc.RA119.008915

Peer reviewed version

Link to published version (if available):
10.1074/jbc.RA119.008915

Link to publication record in Explore Bristol Research
PDF-document

## University of Bristol - Explore Bristol Research
### General rights

# Revising the structure of a new eicosanoid from human platelets to 8,9-11,12-diepoxy-13-hydroxy-eicosadienoic acid

Andrei Kornilov[1], Paul D. Kennedy[1], Maceler Aldrovandi[2], Andrew J.A. Watson[2], Christine Hinz[2], Bryan Harless[1], Joseph Colombo[1], Kirk M. Maxey[1], Victoria J. Tyrrell[2], Matthew Simon[1], Varinder K. Aggarwal[3], William E. Boeglin[4] Alan R. Brash[4], Robert C. Murphy[5], Valerie B. O'Donnell[2]

From [1] Cayman Chemical, 1180 E Ellsworth Rd, Ann Arbor, MI 48108, USA, [2]Systems Immunity Research Institute, School of Medicine, Cardiff University, CF14 4XN, UK, [3]School of Chemistry, University of Bristol, BS6 6RU, UK, [4]Department of Pharmacology and the Vanderbilt Institute of Chemical Biology, Vanderbilt University School of Medicine, Nashville, TN 37232, USA, [5]Department of Pharmacology, University of Colorado, 12801 East 17th Ave, Aurora CO 80045, USA

Running title: *Generation of a diepoxy-eicosanoid by cyclooxygenase-1*

*To whom correspondence should be addressed: Valerie B O'Donnell: Systems Immunity Research Institute, Cardiff University, UK o-donnellvb@cardiff.ac.uk. Or Andrei Kornilov, Cayman Chemical, Ann Arbor, MI 48018, USA. akornilov@caymanchem.com

___

## ABSTRACT

Eicosanoids are critical mediators of fever, pain and inflammation generated by immune and tissue cells. We recently described a new bioactive eicosanoid generated by cyclooxygenase-1 (COX-1) turnover during platelet activation that can stimulate human neutrophil integrin expression. On the basis of mass spectrometry (MS/MS and MS$^3$), stable isotope labeling and GC/MS analysis, we previously proposed a structure of 8-hydroxy-9,11-dioxolane eicosatetraenoic acid (DXA$_3$). Here, we achieved enzymatic synthesis and $^1$H-NMR characterization of this compound with results in conflict with the previously proposed structural assignment. Accordingly, by using LC-MS, we screened autoxidation reactions of 11-HpETE and thereby identified a candidate sharing the precise reverse phase chromatographic and MS characteristics of the platelet product. We optimized these methods to increase yield, allowing full structural analysis by $^1$H-NMR. The revised assignment is presented here as 8,9-11,12-diepoxy-13-hydroxy-eicosadienoic acid, abbreviated to 8,9-11,12-DiEp-13-HEDE or DiEpHEDE, substituted for the previous name DXA$_3$. We found that in platelets, the lipid likely forms via dioxolane ring opening with rearrangement to the diepoxy moieties, followed by oxygen insertion at C13. We present its enzymatic biosynthetic pathway and MS/MS fragmentation pattern, and using the synthetic compound, demonstrate that it has bioactivity. For the platelet lipid, we estimate 16 isomers based on our current knowledge (and 4 isomers for the synthetic lipid). Determining the exact isomeric structure of the platelet lipid remains to be undertaken.

___

**Keywords**: eicosanoid, cyclooxygenase (COX), platelet, lipid, lipid metabolism, immunity, leukocyte-regulating lipid, 8-hydroxy-9,11-dioxolane eicosatetraenoic acid (DXA$_3$), 8,9-11,12-diepoxy-13-hydroxy-eicosadienoic acid (8,9-11,12-DiEp-13-HEDE), DiEpHEDE

Platelets regulate innate immunity during acute infection and injury through their inter-actions with leukocytes (1-3). These cells generate lipid mediators, including eicosanoids such as thromboxane A$_2$ (TXA$_2$), 12-hydroxyeicosatetraenoic acid (12-HETE) and lesser amounts of prostaglandins (PGs) PGE$_2$.

Recently, we examined whether platelets release leukocyte-regulating lipids using a lipidomic approach and uncovered a new eicosanoid formed via COX-1 or COX-2 oxidation of arachidonate (4,5). Based on extensive biochemical evidence including MS/MS of the platelet lipid compared with synthetically generated stable isotope-labelled analogs, the structure of 8-hydroxy-9,11-dioxolane eicosatetraenoic acid (DXA$_3$) was initially proposed. We also used GC/MS, and demonstrated generation of an analogous lipid using purified recombinant COX isoforms. A pathway to chemically synthesized lipid *via* 11-HpETE oxidation was shown, consistent with previous reports for cholesteryl-dioxolanes (6,7). A structure and mechanism of formation was suggested based on our findings. At that time, we

did not have sufficient quantities of purified synthetic lipid for NMR and had to rely on analysis of semi-purified synthetic lipid from low yield reactions only.

To obtain more definitive evidence, we next attempted to generate the proposed dioxolane structure using total synthesis approaches. However, this was not successful. Instead herein, this was achieved through enzymatic oxidation of preformed EETs to form two candidate molecules. However, NMR analysis of these found that dioxolane lipids did not match the platelet isomer. As an alternative strategy, we next focused on modifying and scaling up the chemical oxidation approach to yield a lipid that is consistent with the platelet isomer in terms of MS/MS and reverse phase retention time. We refer to this herein as the "synthetic" lipid (which contains one primary lipid and small amounts of two additional isomers). Once isolated, [1]NMR and COSY analysis was undertaken. The nature of functional groups was revealed, along with position and geometry for both epoxides and one double bond. This data is presented in full herein. In summary, based on our data, the "platelet" lipid is proposed as a further stable metabolite of COX-1, generated likely via ring opening of the dioxolane ring followed by rearrangement and further oxygen insertion. The new structure is presented here as 8,9-11,12-DiEp-13-HEDE (DiEpHEDE), a di-epoxy-monohydroxy eicosadienoic acid, which is generated by COX-1 in human platelets.

## Results

### *Synthesis and purification of DXA₃ from oxidation of EETs*

First, we attempted to generate the proposed structure of DXA$_3$, through oxidation of EETs using a recombinant LOX. In this way, two diastereomers were generated by oxidation of 8S,9R-EET and 8R,9S-EET using recombinant 8*R*-LOX (8) forming specifically the *cis*-endoperoxide product 8S,9S,11R (from 8S,9R-EET) and *trans*-endoperoxide product 8R,9R,11R (from the enantiomer, 8R,9S-EET). ^{1}H-NMR confirmed the structures of these lipids, as shown for the *cis*, 8S,9S,11R, and both showed expected conjugated diene UV spectra (Figure 1, 2). These were then compared using reverse phase LC/MS/MS with the COX-1

derived lipid. However, they eluted later, and while their MS/MS spectra had some common fragment ions (labeled in red), they contained additional large ions that were absent in MS/MS spectra from the COX-1 derived lipid. In particular, these hydroxy-endoperoxides generated large daughter ions at *m/z* 185 quite distinct from the fragmentation properties of the platelet product (Figure 2). Thus these dioxolanes were inconsistent with the platelet lipid and additional candidates were sought as described below.

### *Scaling up generation via arachidonate oxidation, termed "synthetic lipid".*

We previously generated small amounts of the "synthetic lipid", by oxidation of 11-HpETE, as outlined by Porter et al, for synthesizing cholesteryl ester dioxolane derivatives (6,7). This lipid, which has the same MS/MS and reverse phase retention time as the platelet isomer was sufficient for MS/MS analysis, but the produced amounts were not enough to provide good NMR data.

Herein, we modified this method based on observing that the synthetic lipid forms even during the oxidation of arachidonic acid, while making 11-HpETE. In this way, the scaling up was simplified to a single process. Despite the fact that yields were quite low using this method (<0.05%), we managed to isolate the synthetic lipid in the amounts (around 400 μg), which were enough for further analysis. While large numbers of oxidized lipids are present in this crude reaction mixture, only one matched the platelet lipid's MS/MS spectrum and retention time (labeled Peak B in Figure 3). A full description of the purification is presented under Experimental Procedures.

It should be noted that all biologically active eicosanoids would be expected to form at low yield in a complex and uncontrolled free radical oxidation system such as this. If we consider a lipid such as PGE$_2$, we expect that it would be present in such a reaction but at similarly low yield to what we found here, in addition to literally hundreds of other oxidation products.

The lipid matching the platelet lipid based on MS/MS and retention time was targeted for further purification and characterization in this report as follows, and is identified as the synthetic lipid previously characterized in our earlier study(4). Specifically, oxidized lipids

2

were separated using normal phase chromatography, with several products visible at 206 nm (Figure 3 A, labeled A-D). Fractions were collected and analyzed using high resolution Orbitrap MS/MS, and compared to platelet lipid (purified from activated platelets using reverse phase LC). Peak B was found to have the same Orbitrap MS/MS and was further purified using reverse phase HPLC and is thus identified as the synthetic lipid (Figure 3 B,C). Synthetic lipid was next compared with the platelet lipid using a longer UPLC-MS/MS method for further structural confirmation. First, a Q1MS scan of the synthetic lipid shows a prominent peak around 47 min indicating the most abundant component (Figure 4 A). Small peaks eluting immediately before and after are noted, as we previously published for the synthetic lipid generated using 11-HpETE oxidation, and are likely diastereomers (4). Next, both synthetic and platelet lipids were monitored using parent $m/z$ 351.2 fragmenting to daughter ion $m/z$ 165. Again, peak B/synthetic lipid comprises one predominant isomer, with two smaller peaks eluting immediately before and after while the platelet lipid is a single peak (Figure 4 B). These three isomers in the synthetic lipid preparation have identical MS/MS spectra and likely represent quantitatively minor diastereomers of the platelet lipid, as previously reported (data not shown) (4). Importantly, low resolution MS/MS spectra acquired at the apex of the peak at 47.5 min, using a tandem quadrupole instrument are virtually identical (Figure 4 C,D). The synthetic and platelet lipids were next compared using straight phase HPLC. Here, the synthetic lipid shows a slightly later retention time to the platelet isomer (Figure 4 E). This indicates the lipids are likely different stereoisomers of the same compound. Peak B, as purified from Figure 3 B was then taken forward for NMR analysis to inform us about the potential structure of the platelet lipid.

### NMR analysis of synthetic lipid identifies structure as 8,9-11,12-DiEp-13-HEDE

Structure elucidation of synthetic lipid as 8,9-11,12-DiEp-13-HEDE was achieved via ^{1}H-NMR and COSY. For structure numeration and assignment, refer to Figure 5 A,B, 6 A and Table 1. Preliminary determination began with the identification of H13, which was assigned based on the ^{1}H-NMR of a similar compound obtained by Brash(9). Upon identification of the H13

proton, assignment of the epoxide and olefinic protons was possible based on [1]H-^{1}H correlations acquired from the COSY spectrum shown in Figure 6 B, and Table 1. Correlations are observed from H13 to the H14 olefinic proton and to the epoxide proton H12 allowing assignment of these protons. H14 is correlated with the most downfield olefinic proton, which was assigned as H15, and the olefin [1]H-^{1}H coupling of 11Hz confirms that this double bond has the *Z*-configuration (Figure 5 A). This allows the assignment of the peaks between H14 and H15 as the two other olefinic protons. However, protons H5 and H6 are unassigned since their signals appear as multiplets (Figure 5 A). Given the structure of the AA substrate used to generate the synthetic lipid, we propose *cis* geometry for the double bond at 5,6.

These protons are coupled to methylene $CH_2$ protons H4 and H7 (Figure 6B, Table 1). H13 shows correlation to H12 (integrating at ~3.0) at 2.83 ppm, which leaves the single proton at 2.99 ppm to be H11 or H9 (Figure 6B, Table 1). Correlation from the H10 protons to two epoxide protons suggests the final structure as the methylene bridged diepoxide shown (Figure 6 B, 6 C, Table 1). In summary, we propose that both epoxy rings are located in positions 8,9 and 11,12 where the double bonds of AA were originally sited.

Even though assignment of the ^{1}H-NMR and the COSY in $CD_3OD$ allowed us to obtain a general structure, we were interested in gathering additional structural information about the relative stereochemistry of some functional groups in our molecule as was done previously (10). Initial attempts to assign relative stereochemistry between the hydroxyl and 11,12-epoxide via measurement of J couplings were unsuccessful due to the overlap of epoxide protons. Although the synthetic lipid was completely insoluble in benzene, a 90:10 mix of benzene-$d_6$: methanol-$d_4$ was found to yield a proton spectrum in which these epoxide protons were completely separated (Figure 5 B, 6 A). Here, we acquired a proton spectrum that resolved the assignment and J couplings for these. As shown in Figure 5 B, protons in the positions 8 and 9 as well as 11 and 12 contained a small coupling constant in the range of 2.1-2.3Hz which is consistent with *trans*-configuration of epoxy rings(9). Thus, on the basis of the 2 Hz coupling constants, the NMR analysis defines both the 8,9- and 11,12-epoxide groups as *trans*-

epoxy, but their absolute stereochemistry has not been established.

To summarise our NMR data, the synthetic lipid is shown to be 8,9-11,12-diepoxy-13-hydroxy-eicosadienoic acid using NMR and MS/MS. Furthermore, NMR proves the position of the double bond at 14,15, with *cis* geometry. NMR also proves that the relative configuration of the hydroxyl group at 13 and the adjacent carbon atom of epoxy ring at 11,12 is *trans*. Overlapping multiplets for H5 and H6 prevented unambiguous assignment of this double bond configuration. However, based on the structure of AA, we propose that the double bond located at 5,6 has *cis* geometry. Both epoxy rings are confirmed as *trans* configuration. We can't determine the absolute configuration of the hydroxyl group and both epoxy rings from our NMR data. However, the epoxides will be either S,S or R,R, while the hydroxyl will be the same configuration as the epoxy ring at position 11,12. Thus, the list of likely structures for the synthetic lipid includes: 8(*R*),9(*R*)-*trans*-11(*R*),12(*R*)-*trans*-DiEp-13(*R*)-HEDE, 8(*S*),9(*S*)-*trans*-11(*R*),12(*R*)-*trans*-DiEp-13(*R*)-HEDE, 8(*R*),9(*R*)-*trans*-11(*S*),12(*S*)-*trans*-DiEp-13(*S*)-HEDE, 8(*S*),9(*S*)-*trans*-11(*S*),12(*S*)-*trans*-DiEp-13(*S*)-HEDE, with both double bonds predicted as *cis*. With the amount of lipid we were able to generate using our current synhtetic approach, NMR studies are unable to distinguish the absolute configuration further than this. The proposed structure is shown as Figure 6 C, and is also informed by the data in Schneider et al, in which the initial epoxide relative stereochemistry is set via the 9,11-endoperoxide intermediate (9).

***Proposed MS/MS fragmentation for DiEpHEDE***

Overall, our new data showing identical MS/MS and reverse phase retention time to the synthetic lipid generated here confirms the platelet lipid to be 8,9-11,12-diEp-13-HEDE, while different chiral LC retention time indicated that the synthetic and platelet lipids are different isomers. We next considered which candidate isomers are most likely for the platelet lipid. Given the presence of *cis* double bonds in AA, and that COX enzymes generate 13(*R*) hydroperoxyl/hydroxyl isomers during turnover, we predict that the platelet lipid forms in line with these structural features. Given this, we propose that there are 16 potential isomers for the platelet lipid. This is based on the potential for

*cis* or *trans* epoxides and resulting stereochemical configurations possible (Figure 6 D). Unfortunately, a total synthetic approach to generate all 16 would take several years and is beyond the scope of this current study. We note that Schneider previously showed a *cis* epoxide at 9,10, and *trans* at 12,13 for a 8,9-11,12-diEp-13-HEDE isomer generated by a mutant COX-2 isoform (9), however without further evidence for this configuration in the platelet lipid we have not assigned this geometry (see discussion for more detail on this).

Next, based on our findings, the MS/MS fragmentation route previously presented for the platelet lipid, based on extensive high resolution MS/MS of native and deuterated analogs and MS$^3$ was reevaluated. Most daughter ions mapped to similar fragmentation routes, and all major ions could be assigned to this the structure, including *m/z* 195 which could not previously be accounted for (Supplemental Schemes). Possible mechanisms involved in the formation of *m/z* 255, 207, and 163 are presented in Supplemental Scheme 1, as well as mechanisms for *m/z* 333, and 289 (Supplemental Scheme 2), *m/z* 183 and 139 (Supplemental Scheme 3), m/z 195 and 177 (Supplemental Scheme 4), and *m/z* 315 and 271 (Supplemental Scheme 5). All of the proposed reaction pathways taking place in the gas-phase after collisional activation have been previously described for epoxy fatty acids and proposed fragment ions are consistent with the high-resolution mass spectrometric measurements and deuterium labeled analog previously published (4,10).

**8,9-11,12-diEp-13-HEDE** *activates leukocyte integrin expression.*

We previously found that a semi-purified platelet-derived DiEpHEDE isomer can activate neutrophil integrin expression (4). To investigate whether synthetic 8,9-11,12-diEp-13-HEDE retained the same property as the platelet isomer, we repeated the experiment on three separate donor isolates as shown using the synthetic lipid (Figure 7 A, B). In our earlier study, we also found that DiEpHEDE can stimulate priming of neutrophils at far lower amounts of 10 nM. Herein we repeated this several times, but it was not consistent in all donor isolations, being only observed in around 50 %. This suggests reduced potency of the synthetic lipid, and is also consistent with it being a different isomer.

## Discussion

We recently identified a new lipid generated by COX-1 in human platelets that can activate neutrophils and proposed the structure as 8-hydroxy-9,11-dioxolane eicosatetraenoic acid based on extensive biochemical and chemical evidence, but without NMR (4). We now present $^1$H and COSY NMR data, which revises the structure to 8,9-11,12-DiEp-13-HEDE, a metabolite that we suggest forms in platelets through opening of an initially formed dioxolane ring followed by epoxidation, oxygen insertion and reduction as explained in detail below (Figure 6 D). Based both on the biology of COX-1 and structure of the substrate AA, we propose **that** the primary synthetic lipid is one of 4 potential isomers, while the platelet lipid is one of 16, noting that the platelet isomer is not present in the synthetic lipid preparation. This is evidenced by the two lipids having different retention time on chiral phase chromatography (Figure 4 E)

Herein, we tested the ability of the synthetic lipid to either activate (directly) or prime neutrophils in response to the bacterial peptide fMLP, for MAC-1 activation. In the case of priming, the lipid is added first, at far lower concentrations and then the ability of fMLP to activate is tested following a pre-incubation step. In our previous study, we showed that the platelet lipid could activate directly at 10 μM, while it also primed at 10 nM (4). Here, the synthetic lipid showed an ability to activate neutrophils, however for priming it was less effective than we previously observed with the platelet lipid. It is well known that in terms of lipid signalling, isomeric structure is critical to biological function (e.g. recognition by GPCRs). This is similar to prostaglandins and their enantiomers (isoprostanes), which show similarities, but also reduced potency in signalling ability Thus, the synthetic lipid may be less bioactive, leading it to behave differently to the platelet isomer in bioassays at extremely low concentrations. We expect that the amounts of DiEpHEDE generated by platelets will be sufficiently high for signalling at low concentrations. Specifically, we detected generation of around 6 ng/$10^8$ cells, while at the same time there was 1.6ng PGE$_2$ and 25 ng TXB$_2$(4). Importantly, despite lower amounts of PGE$_2$, this lipid is well known to be bioactive towards platelets (11). This indicates that a platelet eicosanoid generated in lower amounts than DiEpHEDE is already known to be

bioactive, providing confidence that DiEpHEDE is generated in biologically-relevant amounts, while noting that generation of this lipid in platelets is sensitive to aspirin(4). While we have not tested the mechanism of action, activation of BLT receptors that are activated by leukotrienes is one possibility.

Lipids generated by vascular cells can possess multiple bioactivities and an exhaustive examination (e.g. vaso constriction, activation of platelets, leukocytes to express integrins, degranulate, mobilise calcium, shape change, phagocytose, aggregate, etc) would be out of the scope of this study.

Previously, we demonstrated that the platelet lipid can be synthesized by COX-1 in intact cells or by recombinant COX-1 or -2 *in vitro* (2). A mechanism was proposed whereby a 9,11-dioxolane lipid with carbon-centered radical at C8 exited the active site then reacted with O$_2$ before reduction to form the product. In those studies, we established that the dioxolane ring forms before lipid exiting the active site using mutant COX-2 enzymes, thus using this information we now present a revised route to formation of 8,9-11,12-diEp-13-HEDE taking this into account as follows (Scheme 1): (i) 9,11-dioxolane with carbon-centered radical at C8 exits active site, (ii) intramolecular attack by the C8 radical on the dioxolane leads to ring opening and reaction by the oxygens on C8 and C12, forming di-epoxides, and leaving a carbon centered radical at C13. This then reacts with O$_2$, before reduction to the 13-hydroxy lipid. While the mechanism in Figure 8 suggests that the lipid radical exits the active site, another possibility is that the second diatomic oxygen attacks while in the active site, similar to the mechanism by which the endoperoxide, PGG$_2$, is formed in the cyclooxygenase pathway. The platelet lipid appears as a single isomer on chiral and reverse phase HPLC, which means that the formation of this lipid is stereochemically controlled. This led us to propose that the dioxolane is formed prior to radical exit.

Formation of di-epoxy-eicosanoids by COX-2 isoforms has been reported previously (9). Thus, we had previously considered these as potential candidates for the platelet lipid. However, they were discounted based on several lines of evidence, in favour of the dioxolane at that time, as follows:

1. Only some mutant COX-2 isoforms have been shown to generate di-epoxy-eicosanoids,

including 8,9-11,12-DiEp-13-HEDE. In previous studies, both wild type COX-2 and the W387F mutant used herein were unable to make the di-epoxide lipid (4,9). As this contrasted with our findings where both could make this new lipid, we considered that specific mutations to the active site are required to enable COX isoforms to facilitate the exit of the dioxolane followed by ring opening and epoxidation. We consider that one potential explanation for our findings was down to the use of different extraction conditions where in this study we may have favoured extraction of more polar products such as these, than in the previous work.

2. During purification of the platelet lipid, a lipid with absorbance suggestive of the presence of a conjugated diene chromophore eluted from the HPLC column (Figure 3 A, B in (4)). This was consistent with the proposed structure of "DXA$_3$", but not with di-epoxides. LC/UV analysis of the purified concentrated DiEpHEDE undertaken for this study confirms no UV active chromophores are present (data not shown). Thus, we have now revisited our raw data from the previous study, and determined that the absorbance most likely originated from a contaminating lipid present in the preparation eluting at the same time, also made by platelets. Specifically, using MS data from biogenic standards we had available at the time of the previous study, we can estimate that the amount of DiEpHEDE eluting in the peak represents around 3.5 μg. However, based on absorbance, the conjugated diene represents only 70 ng of product. Thus, given the amount of platelet lipid eluting, this UV spectrum is too weak to account for the structure proposed.

3. Dioxolane lipids were previously synthesized by Porter's group via oxidation of cholesteryl-11-HpETE (6,7). In our first study, we repeated this reaction using the free acid 11-HpETE as substrate and detected significant amounts of the lipid (4). This provided proof of concept that the 11-hydroperoxyl radical of AA can serve as a precursor for the platelet lipid, under conditions where dioxolanes are known to form *in vitro*. This was consistent with our proposed mechanism of formation via COX isoforms.

Aside from the UV spectrum presented previously (addressed in point 2 above), all our

structural characterization data previously published is directly applicable to the new structure and supports the assignment (4). This extensive data includes derivatization and GC/MS showing one hydroxyl group, no carbonyls, 4 rings/double bonds and two oxygens added to arachidonate(4). Our previous MS/MS and MS$^3$ data including stable isotope labeling studies are re-interpreted to provide new fragmentation pathways, which are fully consistent with the structure and synthesis pathway (Figure 6 D and Supplemental Schemes 1-5). The corrected structure, confirmed to be generated by thrombin activated human platelets by COX-1, and to activate leukocyte integrin expression in vitro is assigned to 8,9-11,12-diEp-13-HEDE.

## Experimental procedures

### Materials

HPLC grade solvents were from Thermo Fisher Scientific (Hemel Hempstead, Hertfordshire, UK). Anti-human CD11b-Alexa Fluor 647 was from BioLegend. All other reagents were from Sigma unless otherwise stated.

### Synthesis of platelet lipid

Human blood donations were approved by the Cardiff University School of Medicine Ethics Committee and were with informed consent (SMREC 12/37, SMREC 12/10), and according to the Declaration of Helsinki. For studies on isolated platelets, whole blood was collected from healthy volunteers free from non-steroidal anti-inflammatory drugs for at least 14 days into acid-citrate-dextrose (ACD; 85 mmol/L trisodium citrate, 65 mmol/L citric acid, 100 mmol/L glucose) (blood:ACD, 8.1:1.9, v/v) and centrifuged at 250$g$ for 10 min at room temperature. Platelet-rich plasma was collected and centrifuged at 900$g$ for 10 min, and the pellet resuspended in Tyrode's buffer (134 mmol/L NaCl, 12 mmol/L NaHCO$_3$, 2.9 mmol/L KCl, 0.34 mmol/L Na$_2$HPO$_4$, 1.0 mmol/L MgCl$_2$, 10 mmol/L HEPEs, 5 mmol/L glucose, pH 7.4) containing ACD (9:1, v/v). Platelets were centrifuged at 800$g$ for 10 min then resuspended in Tyrode's buffer at $2\times10^8$ ml$^{-1}$. Platelets were activated at 37 °C in the presence of 1 mmol/L CaCl$_2$ for 30 min, with 0.2 U ml$^{-1}$ thrombin, before lipid extraction.

*Platelet lipid extraction.*

Lipids were extracted by adding a solvent mixture (1 M acetic acid, 2-propanol, hexane [2:20:30]) to the sample at a ratio of 2.5 ml solvent mixture to 1 ml sample, vortexing, and then adding 2.5 ml of hexane. Following vortexing and centrifugation (300 *g*, 5 minutes), lipids were recovered in the upper hexane layer. The samples were then re-extracted by the addition of an equal volume of hexane followed by further vortexing and centrifugation. The combined hexane layers were then evaporated to dryness using a Rapidvap N2/48 evaporation system (Labconco Corporation) and re-suspended in 200 μl MeOH. Platelet lipid extract was stored at -80 °C until LC/MS/MS analysis.

*Synthesis and purification of lipid matching COX-1 metabolite from platelets.*

Arachidonic acid was mixed with alpha-tocopherol (5% by weight) in the round bottom flask and oxygen was bubbled through this mixture under stirring at 37°C for 3 days. Resulting mixture was purified using flash chromatography on silica gel (hexane:ethyl acetate:acetic acid 90:10:0.5 – 50:50:0.5) and fractions were analyzed using high resolution LC-MS/MS (see Figure 3). Lipids were purified using isocratic separation with a mobile phase of 95:5:0.1 heptane:IPA:acetic acid on a Luna semi-preparative Silica 5μm 250 x 10 mm column at 5 mL/min, monitoring at 206 nm (Figure 3A). A second clean-up step utilized an isocratic separation of 97:2.5:0.5:0.1 heptane:IPA:methanol:acetic acid, with a Luna silica 5 μm 250 x 4.6 mm at 0.5 mL/min, monitoring at 206 nm (Figure 3B).

*Synthesis and purification of 8-hydroxy-9,11-dioxolane eicosatetraenoic acid isomers by LOX oxidation of 8,9-epoxyeicosatetraenoic acids.*

(±)8,9-EET (Cayman) was resolved by semi-preparative chiral HPLC (12), and the enantiomers each reacted with recombinant *P. homomalla* 8*R*-lipoxygenase along the lines described by Teder et al for other lipoxygenase reactions with EETs (13) Briefly, 8,9-EET (50 μM) was reacted in 0.1 M phosphate pH 8 with 8*R*-LOX and the progress followed by UV scanning (200 – 350 nm) with appearance of a conjugated diene chromophore with lambda-max around 240 nm (cf. (13)). Upon complete reaction the products were extracted using a 30 mg Oasis cartridge (Waters), eluted with methanol, and subsequently purified by reversed-phase and normal-phase HPLC. The two main products are an 11*R*-hydroperoxide derivative with the 8,9-epoxide moiety still intact (8,9-epoxy-11*R*-hydroxy-5*Z*,12*E*,14*Z*-eicosatrienoic acid) and the target compound 8-hydroxy-9,11-endoperoxy-5*Z*,12*E*,14*Z*-eicosatrienoic acid. The hydroxy-endoperoxide isomers were generated from both 8*R*,9*S*- and 8*S*,9*R*-EET enantiomers and purified as the methyl ester derivatives for assignment by ^{1}H-NMR. Subsequently, the free acids were isolated and compared by LC-MS with the bioactive platelet product. (For comparison of ^{1}H-NMR and LC data, an equivalent set of derivatives was also prepared by 8*R*-LOX reactions with 5,6-EET, providing 5-hydroxy-6,8-endoperoxy-9*E*,11*Z*,14*Z*-eicosatrienoic acids; these aided in assigning the mass spectral fragmentations of the target hydroxy-endoperoxides derived from 8,9-EET). NMR data on these lipids is provided in Supplementary Data (Supplemental Figure 1).

*NMR methods.*

A Varian Unity Inova 400 MHz or 700 MHz NMR in CD$_3$OD or d-6 Benzene was used for di-epoxy compounds. Post-acquisition processing was performed in ACD/Spectrus processor 2017.2. ^{1}H NMR and ^{1}H,^{1}H COSY NMR spectra on the hydroxy-endoperoxides were obtained on a Bruker 600 MHz spectrometer at 298 K. The parts/million values are reported relative to residual nondeuterated benzene (C6D6; δ = 7.15 ppm) All spectra were analyzed on Bruker TopSpin 3.0 software.

*Straight phase HPLC.*

Lipids were dried then resuspended in mobile phase (hexane: 2-propanol:acetic acid, 90:10:0.1) and injected onto a Chiralcel OD 250 x 4.6mm column (Chiral Technologies Ltd., Exton, PA) with isocratic separation at 1 ml.min-1. Fractions were collected at 30 sec intervals and analysed by direct flow injection monitoring m/z 351.2 to 165.1 on a tandem quadrupole ion trap mass spectrometer (4000 qTrap, Sciex, Thornhill, Canada).

*Reverse-phase LC-MS/MS.*

LC-MS/MS analysis of human platelet-derived and synthetic DiEpHEDE was performed on a Nexera liquid chromatography system (Shimadzu) coupled to by electrospray ionization to a tandem quadrupole ion trap mass

7

spectrometer (4000 qTrap, Sciex, Thornhill, Canada). Briefly, liquid chromatography was performed at 40 °C using a C18 Spherisorb ODS2, 5 μm, 150 × 4.6 mm column (Waters, Hertfordshire, UK) at a flow rate of 1 ml·min$^{-1}$ over 75 min. Mobile phase A was (water, 0.1 % formic acid) and mobile phase B was (acetonitrile, 0.1 % formic acid). The following linear gradient for B was applied: 20 % for 0.5 min, 20 – 42.5 % over 50 min, 42.5 – 90 % from 50 to 60 min, and held at 90 % for 5 min followed by 10 min at initial condition for column re-equilibration. Injection volume was 10 μL. Ionization was performed using electrospray ionization in the negative mode (ESI-), monitoring parent ion to daughter ion *m/z* 351.2 → 165.1 (dwell 200 ms), with the following parameters: TEM 650 °C, GS1 70 psi, GS2 55 psi, CUR 40 psi, ESI spray voltage – 4.3 kV, DP − 53 V, EP − 10 V, CE −26 V and CXP at − 7 V. Full scan MS was carried out in negative mode scanning Q3 from m/z 200 to 600 with total scan time (including pauses) over 4 s. Settings were: TEM 650 °C, GS1 60 psi, GS2 30 psi, CUR 35 psi, ESI spray voltage – 4.5 kV, DP − 55 V, EP − 10 V, CXP at − 30 V and IHE on.

### High resolution LC-MS/MS.

High resolution LC-MS/MS analysis was carried out on an Ultimate 3000 UPLC (Thermo Scientific) coupled to a Q Exactive mass spectrometer (Thermo Scientific). Mass accuracy was determined to be better than 1 ppm. Liquid chromatography was performed using Phenomenex Kinetex C18 , 2.6μm, 100x2.1mm at a flow rate of 400μL·min$^{-1}$ over 25 min. Mobile phases A and B were identical to the method above, but with a gradient for B of 15 – 28 % over 0 to 1 min, 28 – 42% over 1 to 4 min, 42 – 60 % over 4 to 6 min, 60 – 80 % over 6 to 16 min, 80 – 95 % over 16 to 19 min, and held at 95 % over 19 to 22 min followed by 3 min re-equilibration to 15 %. Injection volume 10μL. Electrospray ionization was used in negative mode, with a sheath gas flow rate of 60 units, and capillary temperature at 320 °C. Data dependent MS/MS of *m/z* 351 was carried out with a resolving power of 35,000.

### HPLC-UV analysis of COX-1 derived lipid.

Arachidonic acid was oxidized using recombinant ovine COX-1 in vitro. The enzyme was incubated with two molar equivalents of hematin in 100 mM phosphate buffer for 20 min

on ice. 3.4 μg COX-1 was incubated with 150 μM arachidonate and 500 μM phenol in 100 mM phosphate buffer for 3 min at 37 °C under oxygen atmosphere. Lipids were extracted using the hexane-isopropanol-extraction described above. Lipids from multiple COX-1 reactions were combined and DiEpHEDE was HPLC purified employing a Spherisorb ODS2 column (5 μm, 150 mm x 4.6 mm; Waters) with LC settings and mobile phases described in *Reverse-phase LC-MS/MS*. Fractions were collected every 30 seconds and DiEpHEDE identified by MS/MS monitoring *m/z* 351.2 to 165.1. DiEpHEDE was extracted using solid phase extraction using silica-based solid phase extraction columns (Sep Pak, Waters, MA, USA) which were equilibrated with 5 ml of water pH 3.0 followed by 5 ml of methanol. The DiEpHEDE sample was diluted with water to an organic content of 15 % and purified over the column. The column was washed with 20 ml water at pH 3.0 and the lipid extracted using 5 ml of methanol. Extracts was dried using nitrogen flow and the lipid dissolved in methanol. About 3.5 μg DiEpHEDE was injected on a LC/UV system (Infinity II, Agilent) using the same LC settings and absorbance measured at 235 nm.

### Isolation and activation of human neutrophils

Human neutrophils were isolated from 20 ml citrate anticoagulated whole blood and resuspended in Krebs buffer. Briefly, blood was mixed 1:3 with 2 % trisodium citrate (w/v) and HetaSep (Stemcell technologies) and allowed to sediment for 45 min at 20 °C. The upper plasma layer was recovered and under laid with ice-cold Lymphoprep (2:1 for plasma/Lymphoprep) and centrifuged at 800 *g* for 20 min at 4 °C. The pellet was resuspended in ice-cold PBS and 0.4 % sodium tricitrate (wt/vol) and centrifuged at 400 *g* for 5 min at 4 °C. Contaminating erythrocytes were removed using up to three cycles of hypotonic lysis. Finally, cells were resuspended in a small volume of Krebs buffer (100 mmol/L NaCl, 50 mmol/L HEPES, 5 mmol/L KCl, 1 mmol/L NaH$_2$PO$_4$, 2 mmol/L d-glucose, 1.25 mmol/L MgCl$_2$ and 2 mmol/L CaCl$_2$, pH 7.4), counted and kept on ice. Neutrophils were diluted to $2\times10^6$ cells/ml and incubated in the presence of DiEHEDE or vehicle, for 20 min at 37 °C. In some experiments, neutrophils were pre-incubated with 10 nM DiEpHEDE or vehicle, for 10 min at 37 °C, and then activated with 10 μM fMLP for a

further 10 min at 37 °. Nonspecific antibody binding was blocked using 5 % mouse serum in ice-cold FACS buffer (PBS containing 0.5 % bovine serum albumin (BSA), 5 mmol/L EDTA and 2 mmol/L sodium azide, pH 7.4) for 1 h on ice and centrifuged at 320 $g$ for 5 min at 4 °C. Cells were washed with ice-cold FACS buffer, anti-human CD11b-Alexa Fluor 647 or isotype control added and incubated for 30 min on ice(4). Neutrophils were washed twice with ice-cold FACS buffer and analyzed with a FACSCanto II flow cytometer (BD Biosciences) and FlowJo software.

*Statistics*

Data are expressed as mean ± SEM of three separate determinations. Statistical significance was assessed using one-way ANOVA followed by Bonferroni multiple comparisons test with Prism software version 7 (GraphPad). $p < 0.05$ was considered statistically significant.

**Conflict of Interest:** RCM is a consultant for Avanti Polar Lipids and Cayman Chemical. KMM is President and CEO of Cayman Chemical.

## References

1.  Martinod, K., and Wagner, D. D. (2014) Thrombosis: tangled up in NETs. *Blood* **123**, 2768-2776
2.  Maugeri, N., Campana, L., Gavina, M., Covino, C., De Metrio, M., Panciroli, C., Maiuri, L., Maseri, A., D'Angelo, A., Bianchi, M. E., Rovere-Querini, P., and Manfredi, A. A. (2014) Activated platelets present high mobility group box 1 to neutrophils, inducing autophagy and promoting the extrusion of neutrophil extracellular traps. *Journal of thrombosis and haemostasis : JTH* **12**, 2074-2088
3.  von Bruhl, M. L., Stark, K., Steinhart, A., Chandraratne, S., Konrad, I., Lorenz, M., Khandoga, A., Tirniceriu, A., Coletti, R., Kollnberger, M., Byrne, R. A., Laitinen, I., Walch, A., Brill, A., Pfeiler, S., Manukyan, D., Braun, S., Lange, P., Riegger, J., Ware, J., Eckart, A., Haidari, S., Rudelius, M., Schulz, C., Echtler, K., Brinkmann, V., Schwaiger, M., Preissner, K. T., Wagner, D. D., Mackman, N., Engelmann, B., and Massberg, S. (2012) Monocytes, neutrophils, and platelets cooperate to initiate and propagate venous thrombosis in mice in vivo. *The Journal of experimental medicine* **209**, 819-835
4.  Hinz, C., Aldrovandi, M., Uhlson, C., Marnett, L. J., Longhurst, H. J., Warner, T. D., Alam, S., Slatter, D. A., Lauder, S. N., Allen-Redpath, K., Collins, P. W., Murphy, R. C., Thomas, C. P., and O'Donnell, V. B. (2016) Human Platelets Utilize Cycloxygenase-1 to Generate Dioxolane A3, a Neutrophil-activating Eicosanoid. *J Biol Chem* **291**, 13448-13464
5.  Aldrovandi, M., Hinz, C., Lauder, S. N., Podmore, H., Hornshaw, M., Slatter, D. A., Tyrrell, V. J., Clark, S. R., Marnett, L. J., Collins, P. W., Murphy, R. C., and O'Donnell, V. B. (2017) DioxolaneA3-phosphatidylethanolamines are generated by human platelets and stimulate neutrophil integrin expression. *Redox biology* **11**, 663-672
6.  Yin, H., Brooks, J. D., Gao, L., Porter, N. A., and Morrow, J. D. (2007) Identification of novel autoxidation products of the omega-3 fatty acid eicosapentaenoic acid in vitro and in vivo. *The Journal of biological chemistry* **282**, 29890-29901
7.  Yin, H., Morrow, J. D., and Porter, N. A. (2004) Identification of a novel class of endoperoxides from arachidonate autoxidation. *The Journal of biological chemistry* **279**, 3766-3776
8.  Gilbert, N. C., Neau, D. B., and Newcomer, M. E. (2018) Expression of an 8R-lipoxygenase from the coral *Plexaura homomalla*. *Methods Enzymol.* **605**, 33-49
9.  Schneider, C., Boeglin, W. E., and Brash, A. R. (2004) Identification of two cyclooxygenase active site residues, Leucine 384 and Glycine 526, that control carbon ring cyclization in prostaglandin biosynthesis. *J Biol Chem* **279**, 4404-4414
10. Murphy, R. C. (2015) New Developments in Mass Spectrometry. in *Tandem Mass Spectrometry of Lipids: Molecular Analysis of Complex Lipids* (Gaskell, S. ed.), Royal Society of Chemistry, London, UK. pp
11. Smith, J. P., Haddad, E. V., Downey, J. D., Breyer, R. M., and Boutaud, O. (2010) PGE2 decreases reactivity of human platelets by activating EP2 and EP4. *Thromb Res* **126**, e23-29
12. Schneider, C., Boeglin, W. E., and Brash, A. R. (2000) Enantiomeric separation of hydroxy eicosanoids by chiral column chromatography: effect of the alcohol modifier. *Anal. Biochem.* **287**, 186-189
13. Teder, T., Boeglin, W. E., and Brash, A. R. (2014) Lipoxygenase-catalyzed transformation of epoxy fatty acids to hydroxy-endoperoxides: a potential P450 and lipoxygenase interaction. *J. Lipid Res.* **55**, 2587-2596

**FOOTNOTES**

The abbreviations used are: $DXA_3$, 8-hydroxy-9,11-dioxolane eicosatetraenoic acid; 8,9-11,12-DiEp-13-HEDE or DiEpHEDE, 8,9-11,12-diepoxy-13-hydroxy-eicosadienoic acid; COX, cyclooxygenase; TX, thromboxane; HETE, hydroxyeicosatetraenoic acid.

| F2 axis (ppm) | F1 axis (ppm) | Correlation |
|---|---|---|
| 1.33 | 0.89 | H20-19 |
| 1.38 | 1.33 | H18-17 |
| 1.65 | 2.29 | H3-2 |
| 1.66 | 2.08 | H4-3 |
| 1.92 | 1.76 | H10'-10'' |
| 2.1 | 1.38 | H17-16 |
| 2.83 | 2.29 | H8-7 |
| 2.84 | 1.93 | H10'-9 |
| 2.84 | 1.76 | H10''-9 |
| 3.00 | 1.90 | H11-10' |
| 3.00 | 1.76 | H11-10'' |
| 4.41 | 2.84 | H13-12 |
| 5.35 | 4.39 | H14-13 |
| 5.48 | 2.29 | H7-6 |
| 5.51 | 2.09 | H5-4 |
| 5.61 | 5.35 | H15-14 |
| 5.62 | 2.08 | H16-15 |

**Table 1. COSY assignment of 8,9-11,12-DiE-13-HEDE ^{1}H-^{1}H  gDQCOSY (METHANOL-*$d_4$*, 400 MHz)**
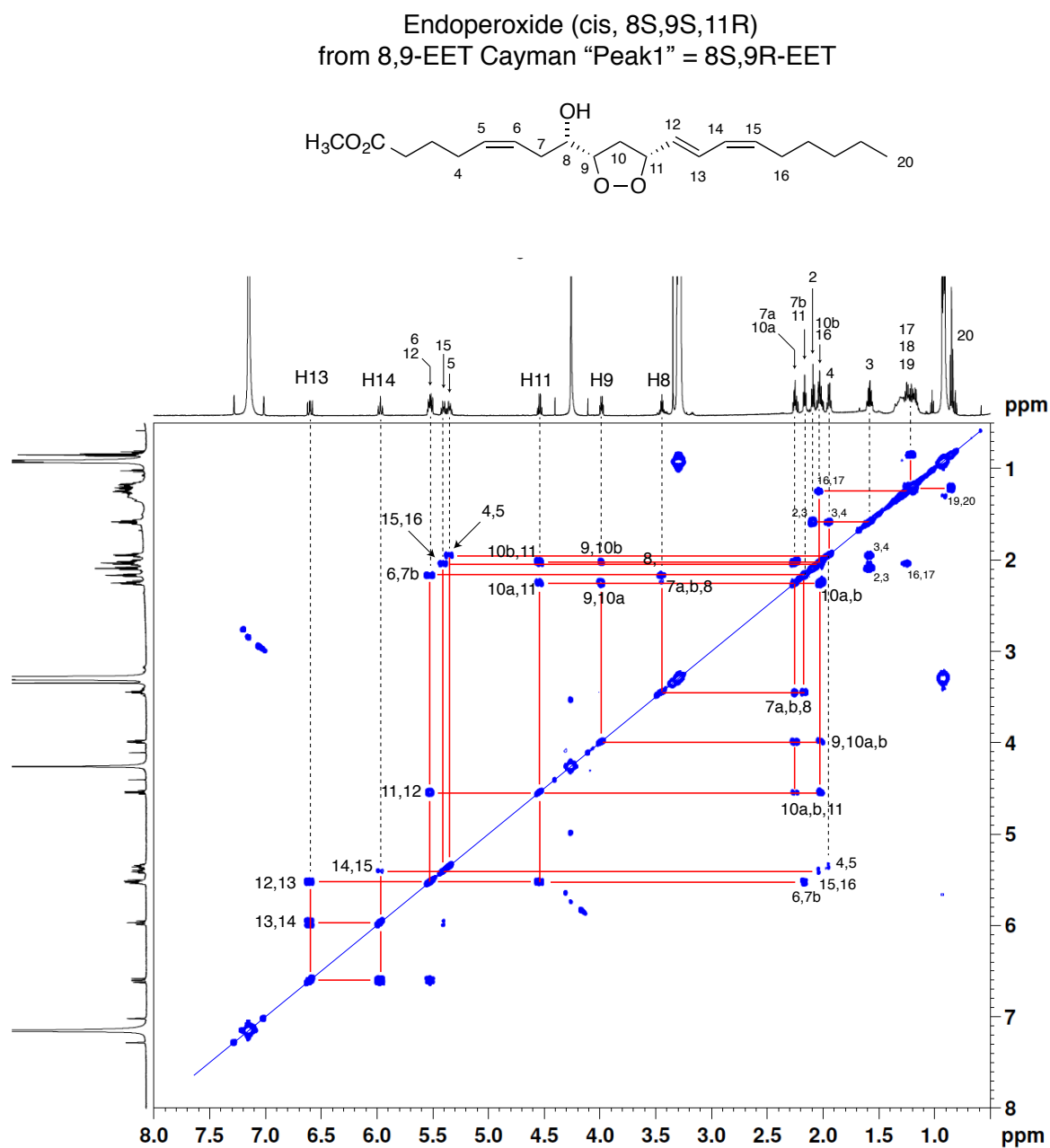
**Figure 1.** **¹H-NMR spectrum and COSY analysis of 8*S*-hydroxy-9*S*,11*R*-endoperoxy-5*cis*,12*trans*,14*cis*-eicosatrienoate Me ester in d6-benzene**

13
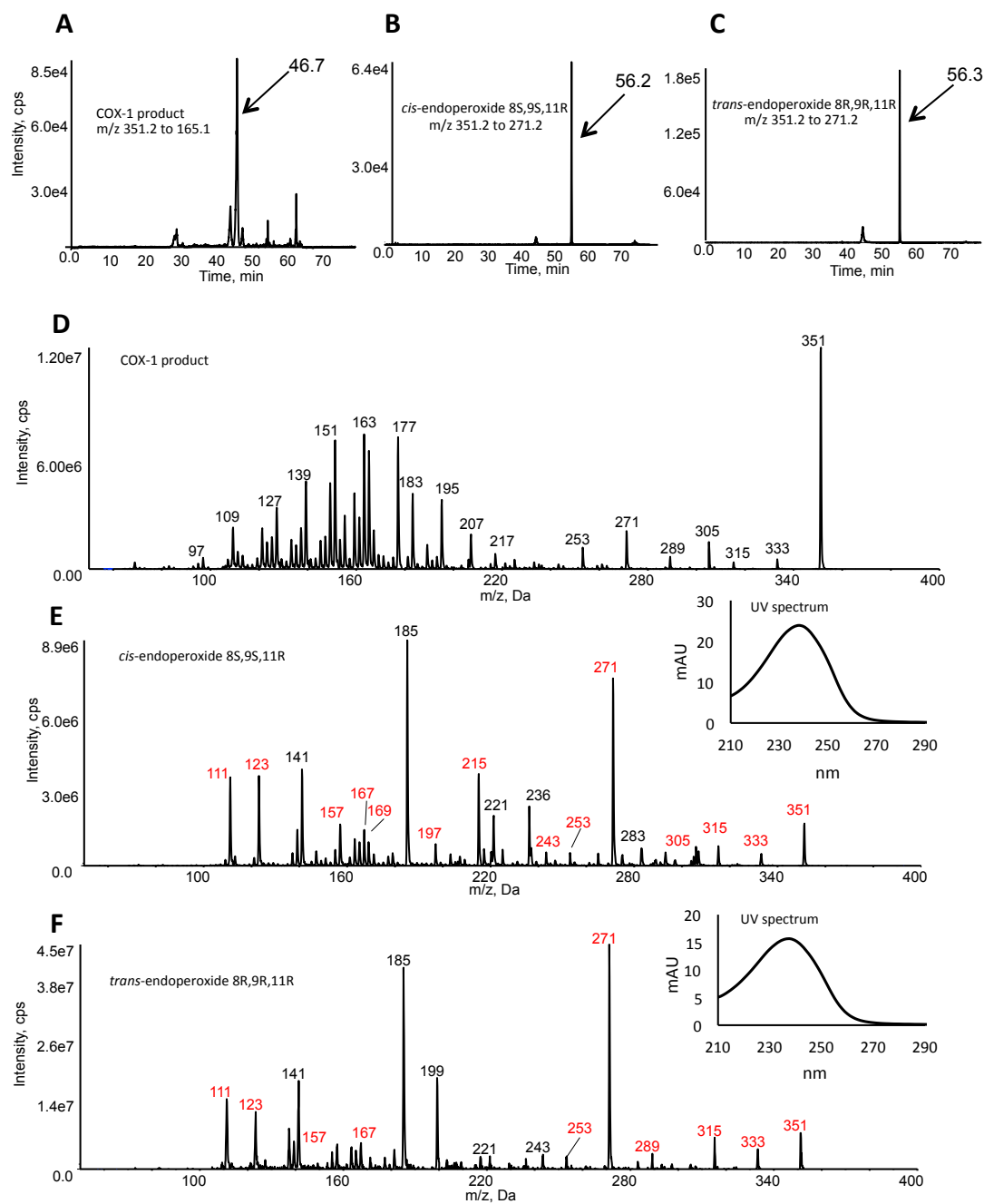
**Figure 2. Comparison of the COX-1 derved lipid with 8-hydroxy-9,11-dioxolanes indicates these are different lipids.** *Panels A-C. Reverse phase LC/MS/MS indicates that the lipids elute at different retention times.* Lipids (COX-1 product, or 8-hydroxy-9,11-dioxolanes were separated using reverse phase LC/MS/MS as described in Methods and compared for retention time. Lipids were detected either as m/z 351.2 to 165.1 (COX-1 lipid) or to 271.1 (dioxolanes). *Panels D-F. Comparison of MS/MS spectra from the COX-1 derived lipid versus in vitro generated dioxolanes, along with confirmation of conjugated diene structures for dioxolanes.* MS/MS spectra were acquired at the peak of elution for the lipids shown in Panels A-C above. Ions shown in red for E, F are common to the COX-1 product. Nominal mass is shown as these are low resolution spectra (tandem quadruploe mass spectrometer). Inset UV spectra for the dioxolanes were obtained by HPLC-UV analysis as indicated in Methods.
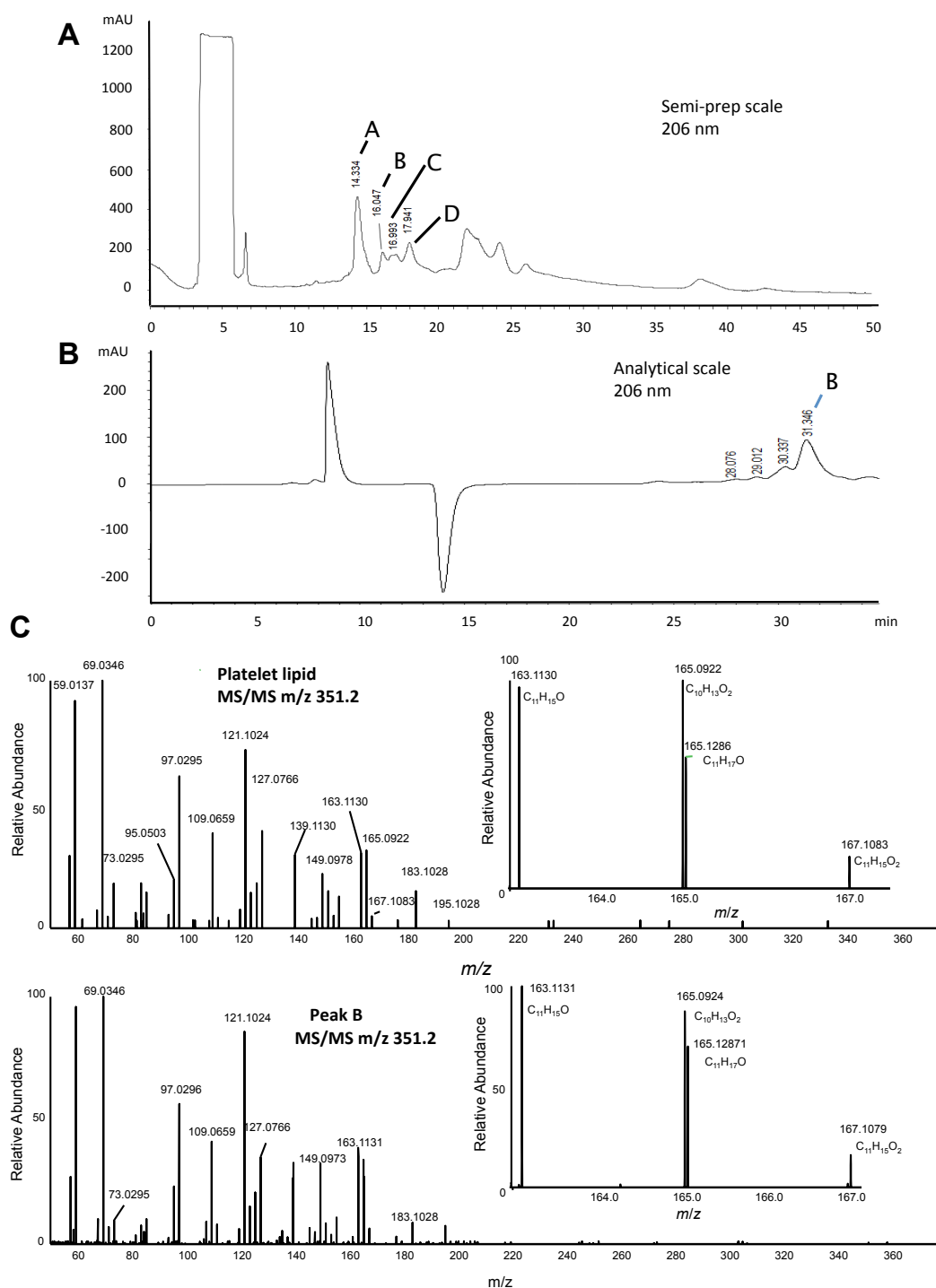
14

**Figure 3. Purification and high resolution MS of lipids generated by oxidation of arachidonate, to isolate the synthetic lipid**. *Panel A*. Semi prep normal phase HPLC, as indicated in Methods, with collected fractions labeled A-D. The HPLC was monitored online at 206 nm. *Panel B*. Further HPLC purification of peak B (Figure 1A), as indicated in Methods. The HPLC was monitored online at 206 nm. *Panel C*. High resolution (Orbitrap) LC-MS/MS of platelet lipid (top) versus Peak B (bottom), as indicated in Methods.
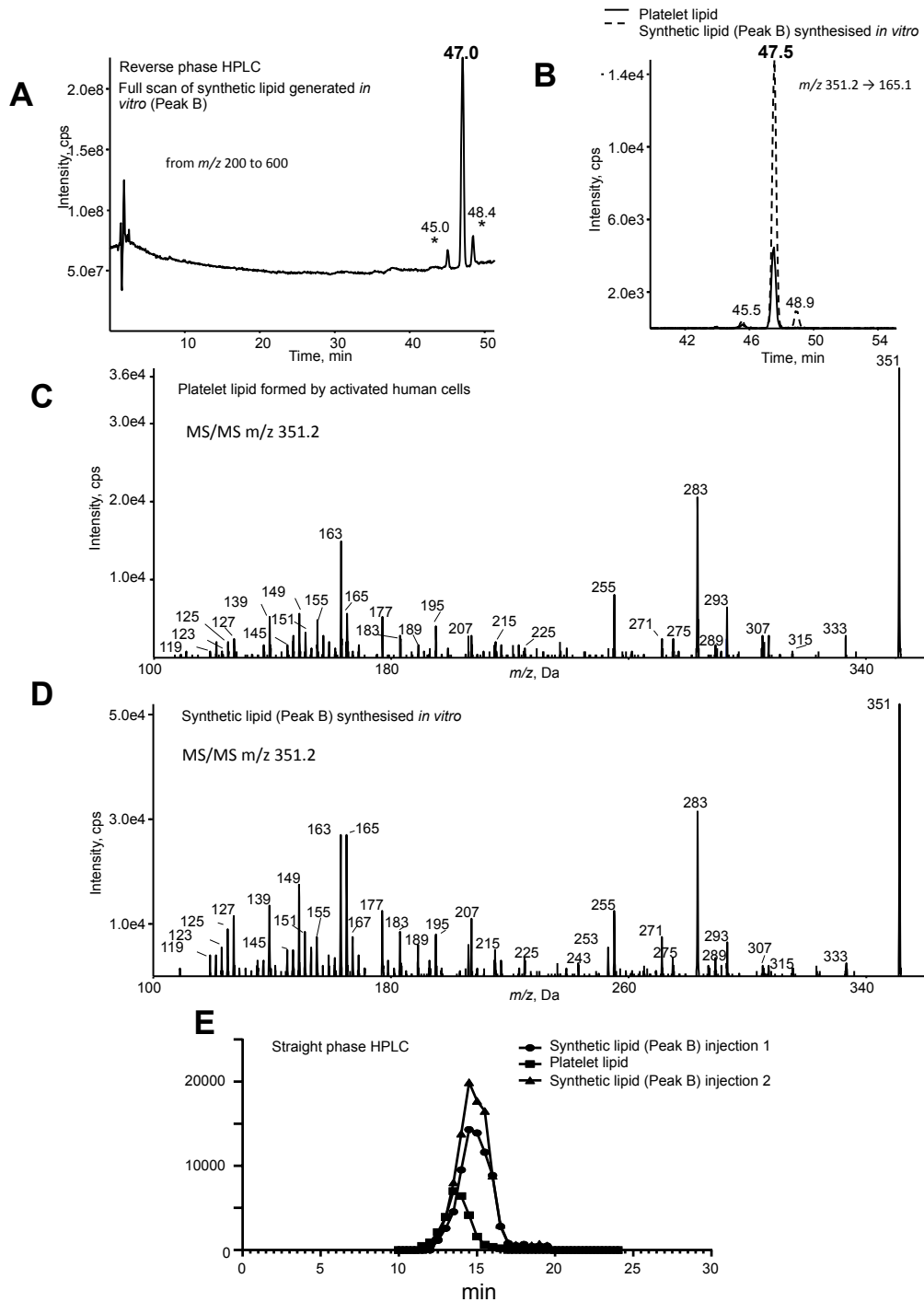
**Figure 4. Analysis of platelet lipid and Peak B confirms them to be isomers of the same lipid structure.** Washed human platelets were activated with 0.2 unit·ml$^{-1}$ thrombin, for 30 min at 37 °C, and lipids extracted. Peak B was generated *in vitro* and purified as described in Methods. *Panel A. Purified Peak B was analysed using reverse phase LC/MS/MS on the tandem quadrupole, in full scan mode.* Full scan was carried out in negative mode, scanning Q3 from *m/z* 200 to 600. * shows position of additional isomers of Peak B. *Panel B. Reverse phase LC/MS/MS of platelet lipid and Peak B showing co-elution.* Lipids were analyzed using reverse phase LC/MS/MS, monitoring parent *m/z* 351.2 → 165.1. *Panels C,D. MS/MS spectra of the lipids obtained with a tandem qudrupole mass spectrometer.* Lipids were separated as in *B* and MS/MS spectra acquired at the apex of elution using enhanced product ion mode. Nominal mass is shown as these are low-resolution spectra. *Panel E. Straight phase HPLC of platelet lipid and Peak B show the lipids separate.* Lipids were resuspended in mobile phase and analysed as outlined in Methods.
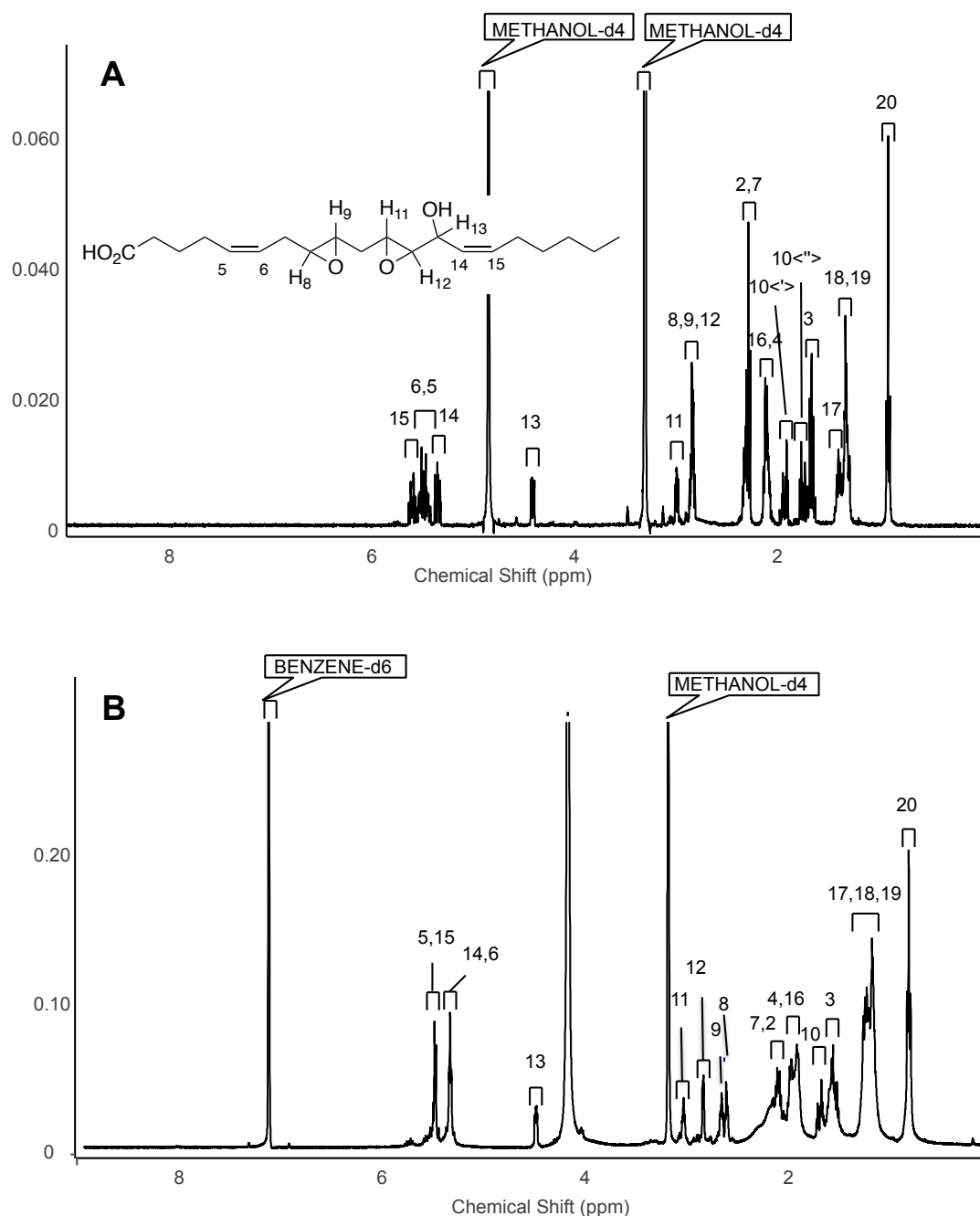
**Figure 5. H-NMR data of the synthetic lipid in Methanol-d₄ and Benzene-d₆ shows the structure as 8,9-11,12-DiEp-13-HEDE.** *Panel A.* ^{1}H NMR (METHANOL-$d_4$, 400 MHz) δ 5.60 (dtd, 1H, *J*=1.17, 7.54, 11.08 Hz), 5.48 (m, 2H), 5.35 (tdd, 1H, *J*=1.56, 8.59, 10.94 Hz), 4.41 (ddd, 1H, *J*=1.17, 4.10, 8.79 Hz), 2.97-3.00 (m, 1H), 2.86-2.81 (m, 3H), 2.34-2.31 (m, 2H), 2.28 (t, 2H, 7.23 Hz), 2.13-2.07 (m, 4H), 1.95-1.89 (m, 1H), 1.77-1.71 (m, 1H), 1.66 (qint, 2H, 7.23 Hz), 1.41-1.36 (m, 2H), 1,31-1.28 (br m, 4H), 0.90 (t, 3H, 7.0 Hz). *Panel B.* ^{1}H NMR (BENZENE-d6/METHANOL-d4 90:10, 700 MHz) δ 5.51-5.43 (m, 2H), 5.36-5.29 (m, 2H), 4.48 (dd, 1H, *J*=7.75, 4.0 Hz), 3.03 (dt, 1H, *J*=2.20, 5.1 Hz), 2.83 (dd, 1H, *J*=2.13, 3.83 Hz), 2.65 (dt, 1H, *J*=2.25, 5.20 Hz), 2.61 (dt, 1H, *J*=2.21, 5.36 Hz), 2.14-2.05 (m, 2H), 2.02-1.85 (m, 4H), 1.72-1.63 (dt, 1H, J=15.03, 4.58 Hz), 1.58-1.48 (m, 3H), 1.31-1.10 (m, 8H), 0.81 (t, 3H, *J*=6.9 Hz)
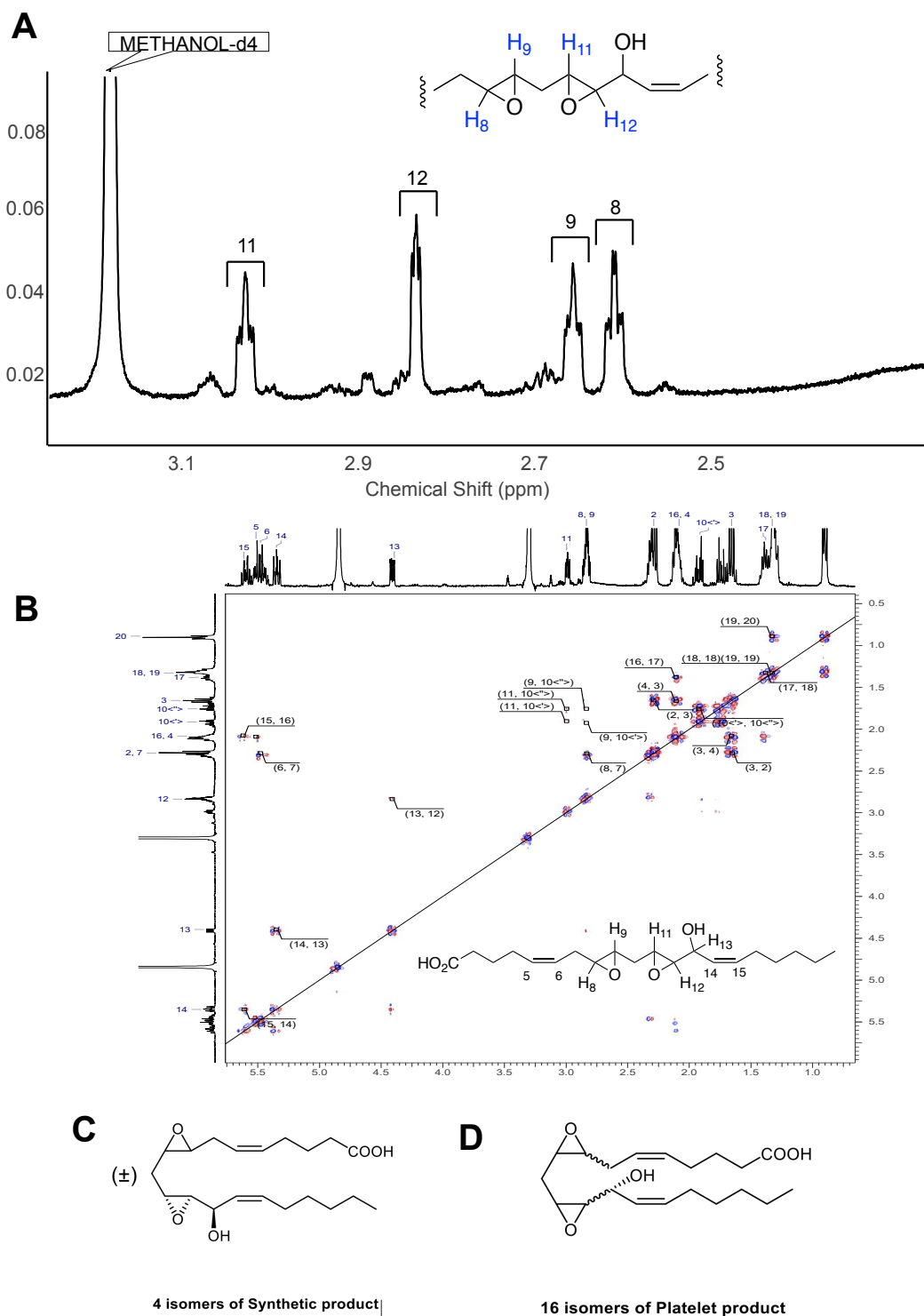
17

**Figure 6. H-NMR data of the synthetic lipid continued** *Panel A. Region of epoxy protons* ^{1}H NMR (BENZENE-d6/METHANOL-d4 90:10, 700 MHz) δ 3.04-3.01 (dt, 1H, *J*=2.20, 5.1 Hz), 2.84-2.83 (dd, 1H, *J*=2.13, 3.83 Hz), 2.66-2.64 (dt, 1H, *J*=2.25, 5.20 Hz), 2.62-2.60 (dt, 1H, *J*=2.21, 5.36 Hz) *Panel B. 2D COSY. Panel C Structure of the synthetic generated diEHEDE isomer.* (±)8,9-*trans*-11(*R*),12(*R*)-*trans*-DiEp-13(*R*)-HEDE. *Panel D. Structure of the proposed platelet lipid 8,9-11,12-DiEp-13-HEDE.* Shown here is the isomer proposed based on studies using mutant COX-2 isoforms: 8(*R*),9(*R*)-*cis*-11(*R*),12(*R*)-*trans*-diEp-13(*R*)-HEDE.
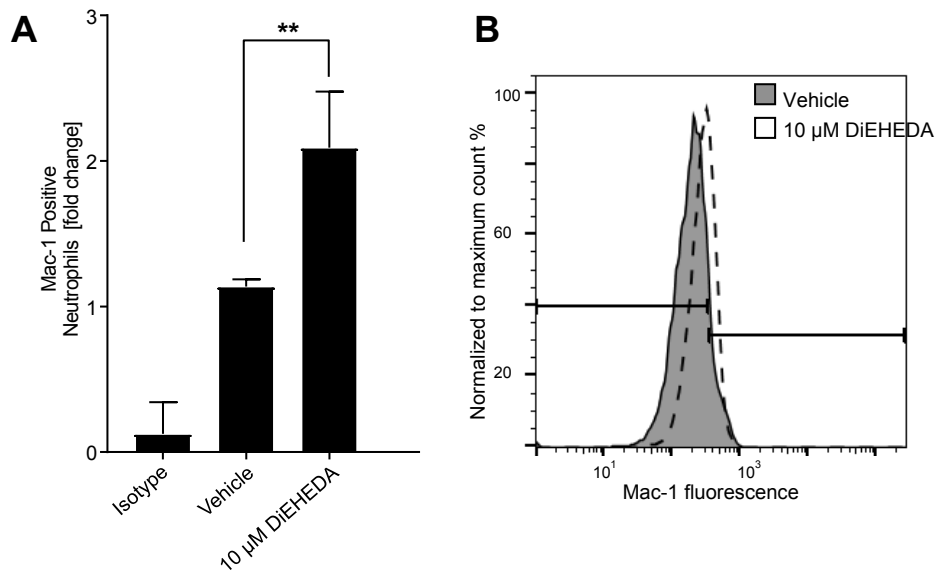
18

**Figure 7. DiEpHEDE activates neutrophil Mac-1 expression.** *Panel B. DiEpHEDE activates human neutrophil Mac-1 expression.* Neutrophils were incubated with synthetic DiEpHEDE or vehicle, for 20 min at 37 °C, and Mac-1 expression monitored by flow cytometry using anti-human CD11b (Mac-1)-Alexa Fluor 647. Where stated, neutrophils were pre-incubated with 10 µM synthetic DiEpHEDE or vehicle for 10 min at 37 °C, and then activated with 10 µM fMLP for a further 10 min at 37 °C. *Panel A.* Bar chart showing activation of Mac-1 expression by DiEpHEDE . Data represent fold change in fluorescent signal normalized to vehicle control (n = 3 mean ± SEM). Statistical significance used one-way ANOVA followed by Bonferroni Post Hoc Test,*, $p < 0.05$. *Panel B.* Representative histogram depicting increased Mac-1 expression following activation with DiEpHEDE. Line represents the Mac-1-positive neutrophil gate, as set using untreated neutrophils.
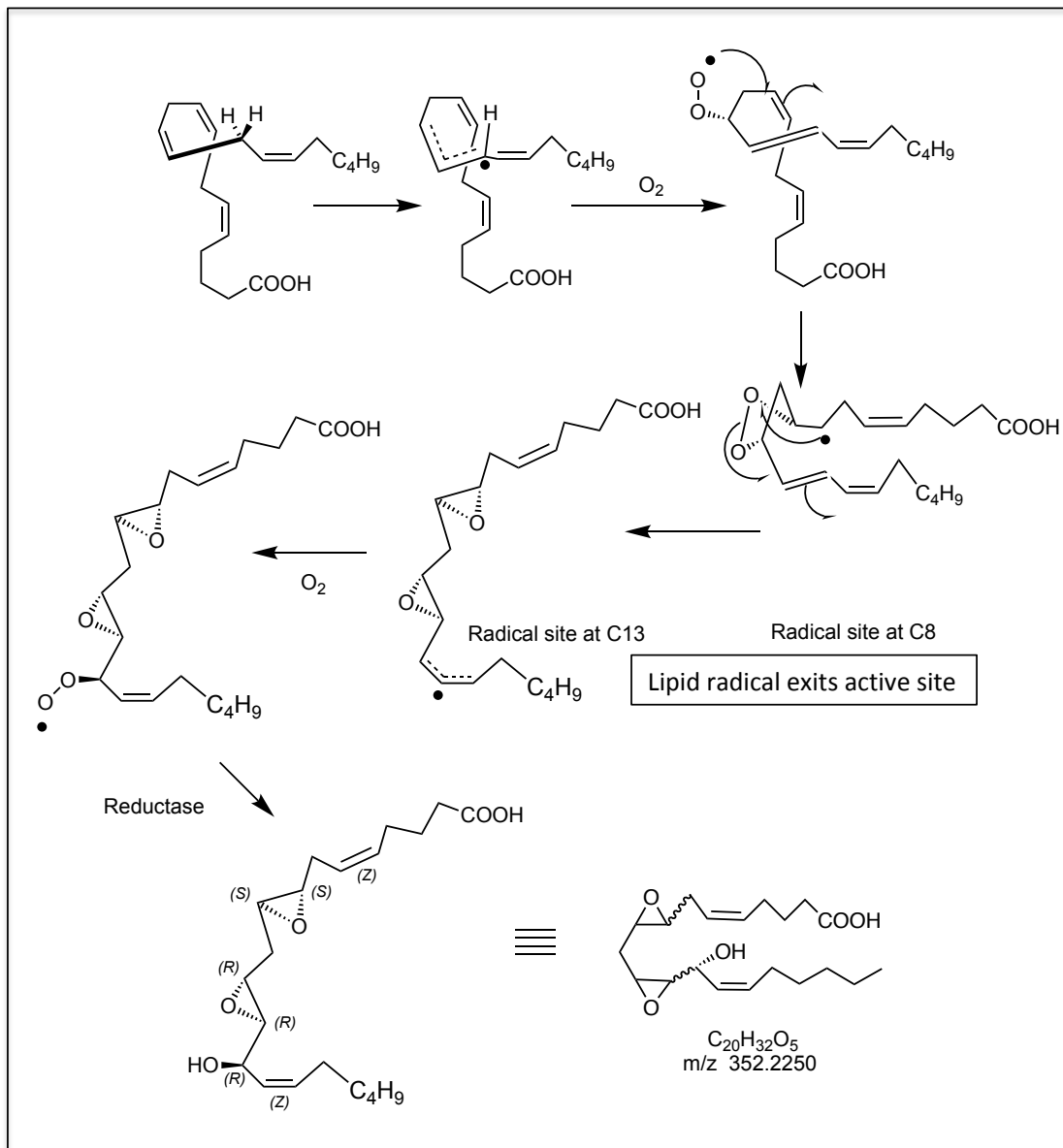
**Figure 8. Proposed route to synthesis of 8,9-11,12-DiEp-13-HEDE by COX isoforms.**